JOURNAL OF Materials CHEMISTRY

# The structure of $Cd_2Os_2O_7$ through the metal–semiconductor transition by powder neutron diffraction

**Jonathan Reading and Mark T. Weller***

*Department of Chemistry, University of Southampton, Southampton, Hants, UK SO17 1BJ. E-mail: mtw@soton.ac.uk*

***Received 13th March 2001, Accepted 6th June 2001***
***First published as an Advance Article on the web 2nd August 2001***

Samples of non-absorbing $Cd_2Os_2O_7$ have been studied using powder neutron diffraction over the temperature range 12–298 K. Lattice parameters show a discontinuity at $T_{MI}$ (225 K) consistent with the transition from low temperature semiconducting to metallic behaviour. Changes in structural features occur in the range 12–225 K with a decrease in the Os–O bond lengths and formation of slightly more regular $OsO_6$ octahedra. No evidence of long range magnetic ordering was observed down to 12 K.

## Introduction

The pyrochlore structure is a common structure type adopted by materials of the composition $A_2M_2O_{7-x}$ where A is a larger mono-, di- or trivalent cation and M is smaller tetra-, penta- or hexavalent cation. Examples include $Pb_2Nb_2O_7$, $Nd_2Ru_2O_7$ and $Bi_2Sn_2O_7$. The structure can be considered as being derived from a fluorite structure with the composition $[A_2M_2]O_8$ by the removal of two oxide anions in a regular fashion producing, $A_2M_2O_7\square$, where $\square$ represents a vacancy. Alternatively the structure can be viewed as consisting of $MO_6$ octahedra sharing all vertices with a distorted (6+2) cubic co-ordination to A, Fig. 1. A review of the pyrochlore system, describing the wealth of materials adopting this structure type and their properties, has been published by Subramanian *et al.*[1] Most recent activity in pyrochlore chemistry has been focussed on the magnetic and electronic properties of those materials of this family containing transition elements as the M-type cation. For example, the ruthenium(IV) pyrochlores, such as $Ln_2Ru_2O_7$ and $Y_2Ru_2O_7$, and the titanium(IV)-containing materials $Ln_2Ti_2O_7$ have been investigated in terms of their magnetic structures and magnetic frustration by a number of groups.[2–4] Further attention has been focussed on $Tl_2Ru_2O_7$, which exhibits strong magnetoresistive effects.[5,6]

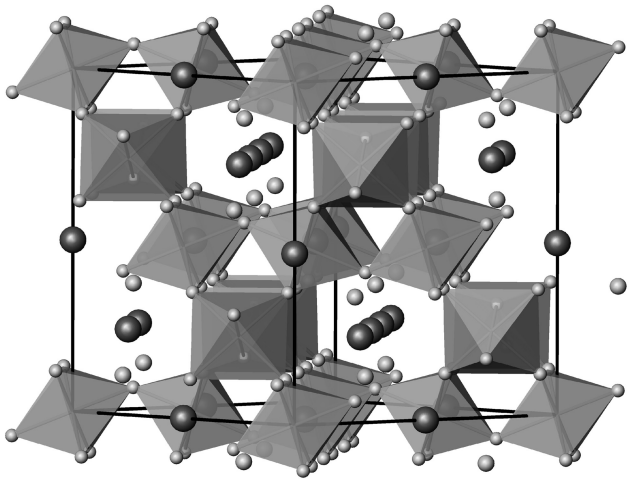

**Fig. 1** The pyrochlore structure shown as linked $OsO_6$ octahedra surrounding Cd (large darker spheres) and O (small, paler unlinked spheres)

One of the pyrochlores originally reported by Sleight *et al.*[7] as part of a systematic study in the early 1970s of materials with this structure type was the more unusual (2+,5+) material $Cd_2Os_2O_7$. This compound, studied as single crystals, was found to exhibit an electronic second order metal–semiconductor/insulator transition at 225 K, $T_{MI}$, with associated antiferromagnetic ordering. The low temperature resistive behaviour was interpreted in terms of a slow collapse of a semiconductor band gap to zero, while the high temperature resistive behaviour was unusual in exhibiting a very small increase with temperature. It is of note that while two different crystals demonstrated similar low temperature resistivity behaviour between 225 and 150 K, below 150 K marked variations occurred. Magnetic susceptibility measurements show clear antiferromagnetic ordering at 225 K; the high temperature behaviour in the metallic state is atypical and not fitted by a Curie–Weiss expression. Investigations of the $Cd_2Os_2O_7$ structure at room temperature and 77 K using single crystal X-ray methods showed no difference, in terms of lower symmetry, or peak broadening effects. However, single crystal X-ray methods are not ideal for the investigation of such structure variations in this material for a number of reasons. Firstly, single crystal methods are poor at resolving small changes in lattice parameters, due to the limited angular range of the diffraction data and, secondly, X-ray methods are insensitive to oxygen positions in such heavy metal oxides. The method of choice in investigating the structure of $Cd_2Os_2O_7$ is neutron diffraction; this technique can also supply information on any long range magnetic ordering occurring in the structure. However, natural cadmium (containing 12% $^{113}Cd$) is an extremely strong absorber of neutrons, making investigation of the structures of materials containing moderate levels of cadmium using neutron methods impossible. Nevertheless, some isotopes of cadmium have negligible neutron absorption characteristics, *e.g.* $^{114}Cd$, making material containing one of these isotopes alone suitable for neutron diffraction work.

In this article we report a study of the structure of $^{114}Cd_2Os_2O_7$ using powder neutron diffraction over the temperature range 12 to 298 K, defining the changes in structure that occur as a function of temperature. We also report a lack of evidence for long range magnetic ordering in this structure, presumably as a result of magnetic frustration in the pyrochlore framework.

## Experimental

Samples of $Cd_2Os_2O_7$ were prepared by grinding together high purity stoichiometric mixtures of CdO (99.9%), Os (99.8%) and $OsO_4$ (99.95%). As $^{113}Cd$ is a highly absorbing isotope (absorption cross-section $= 2.06 \times 10^{-20}$ cm$^2$),[8] natural abundance CdO (containing *ca.* 12% $^{113}Cd$) could not be used if good quality data was to be obtained. A $^{114}Cd$ (absorption cross-section $= 3.40 \times 10^{-25}$ cm$^2$)[8] enriched sample of CdO was used (99% $^{114}Cd$, Trace Sciences International). The mixture was loaded into a silica ampoule and sealed under vacuum with the sample end immersed in liquid nitrogen to avoid osmium loss due to the volatility of $OsO_4$. The mixture was heated at 800 °C for 1 day, then cooled and the silica ampoule opened. The product at this stage was reground, resealed and heated to 800 °C for a further 3 days. Powder X-ray diffraction data were recorded on the black product using a Siemens D5000 diffractometer operating with Cu-K$\alpha_1$ radiation. The pattern was consistent with phase-pure pyrochlore product material, cubic $a = 10.17$ Å, with the exception of a small trace of $OsO_2$ ($I/I_0 < 2\%$).

### Powder neutron diffraction

Time of flight (TOF) powder neutron diffraction data were collected on the POLARIS diffractometer at the Rutherford Appleton Laboratory, Oxfordshire, UK The experiment was carried out using a closed cycle refrigeration (CCR) system at a series of temperatures, ranging from 12 K to room temperature. Data were collected for 75 min at each temperature with the exception of those around the transition (200–230 K), room temperature and 12 K, which were run for 135, 210 and 190 min, respectively. The room temperature data set was collected initially, followed by cooling to 12 K and staged heating back to 250 K.

Rietveld refinement of structure was undertaken using GSAS[9] and employed the cubic pyrochlore model in the space group $Fd\bar{3}m$. For these refinements, only the back-scattering bank data was used, with times-of-flight ranging from 3000 to 19500 μs, corresponding to the *d*-spacing range 0.5–3.1 Å. A uniform approach to the structure refinement was undertaken for each of the data sets obtained at different temperatures, to ensure consistent results. Cell parameters, peak shape parameters atomic positions and isotropic temperature factors were sequentially added to the refinement. The scattering length for the $^{114}Cd$ isotope was taken as 7.5 fm.[8] The fractional occupancies of the oxygen positions were investigated for site deficiency but all values refined to full occupancy within esds. Refinement of the osmium site occupancy showed no deviation from unity. For cadmium, a small deficiency could be refined but this was associated with a strongly correlated reduction in isotropic displacement parameter and statistically insignificant improvement in profile fit factors; the cadmium occupancy was therefore fixed at unity. The small level of $OsO_2$ impurity (*ca.* 2%) was modelled to improve the overall final profile fit. The final stages of the refinement included anisotropic temperature factors for all atoms. For each data set the refinement converged smoothly. Fig. 2 shows the (typical) fit obtained to the room temperature data. Derived lattice parameters, atomic co-ordinates, displacement factors ($100U_{eq}$) and profile fit parameters at each temperature are summarised in Table 1, together with the crystallographic description of the structure. Fit parameters and $\chi^2$ values show behaviour in line with the data collection times.

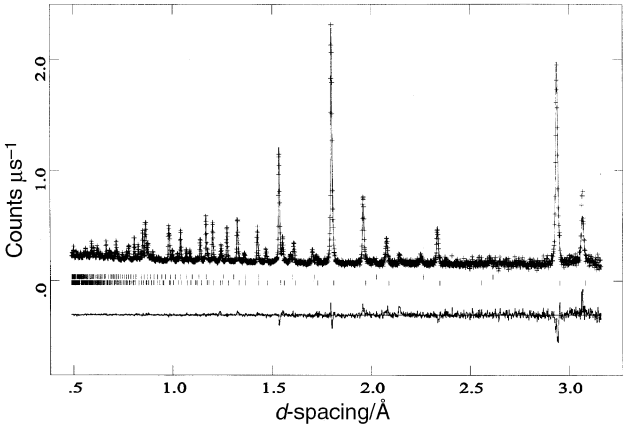


**Fig. 2** Example of the fit achieved to powder diffraction data at $T = 300$ K. Crosses are experimental points, the upper continuous line the calculated profile and the lower continuous line the difference. Tick marks show reflection positions: $Cd_2Os_2O_7$ (lower) and $OsO_2$ (upper).

## Results

### Atomic structure

Fig. 3 shows the variation in the lattice parameter as a function of temperature. A smooth increase, attenuated at the lowest temperatures, is seen between 12 K and 220 K consistent with characteristic thermal expansion. Over the range 100–200 K the thermal expansion co-efficient is $3.8 \times 10^{-5}$ Å K$^{-1}$, typical of a framework oxide; a similar rate of thermal expansion is seen above 230 K. A clear inflection is seen in the lattice parameter at the semiconductor–metal transition temperature that is presumably associated with the delocalisation of the electrons and abrupt change in resistive behaviour (3 to 4 orders of magnitude drop in resistivity).[7] This decrease in lattice constants on approaching $T_{MI}$ is similar to those observed in some other metal–insulator transition materials such as $SmNiO_3$[10,11] In this compound, the electron delocalisation leads to a clear decrease in all the Ni–O distances. For

**Table 1** Summary of derived atomic, thermal and profile fit parameters for $Cd_2Os_2O_7$ as a function of temperature; esds are given in parentheses. Space group $Fd\bar{3}m$. Cd on (1/2,1/2,1/2), Os on (0,0,0), O1 on ($x$,1/8,1/8) and O2 on (3/8,3/8,3/8)

| $T$/K | $a$/Å | O1 $x$ | Cd $U_{eq} \times 100$/Å$^2$ | Os $U_{eq} \times 100$/Å$^2$ | O1 $U_{eq} \times 100$/Å$^2$ | O2 $U_{eq} \times 100$/Å$^2$ | $R_{wp}$ (%) | $R_p$ (%) | $\chi^2$ |
|---|---|---|---|---|---|---|---|---|---|
| 12.0 | 10.16043(5) | 0.32078(7) | 0.89(3) | 0.02(1) | 0.31(2) | 0.33(2) | 2.73 | 5.41 | 2.31 |
| 50.0 | 10.16078(7) | 0.32072(8) | 0.94(3) | 0.04(1) | 0.32(2) | 0.33(2) | 3.26 | 6.88 | 1.37 |
| 75.0 | 10.16139(7) | 0.32064(9) | 1.01(3) | 0.06(1) | 0.34(2) | 0.35(2) | 3.30 | 7.03 | 1.30 |
| 100.0 | 10.16227(7) | 0.32069(9) | 1.08(3) | 0.08(1) | 0.38(2) | 0.44(2) | 3.28 | 6.92 | 1.29 |
| 125.0 | 10.16324(7) | 0.32058(9) | 1.15(3) | 0.08(1) | 0.40(2) | 0.41(2) | 3.35 | 7.11 | 1.31 |
| 150.0 | 10.16414(7) | 0.32055(9) | 1.21(3) | 0.11(1) | 0.45(2) | 0.46(2) | 3.22 | 7.12 | 1.21 |
| 175.0 | 10.16511(7) | 0.32035(9) | 1.33(3) | 0.12(1) | 0.51(2) | 0.51(2) | 3.21 | 7.09 | 1.22 |
| 200.0 | 10.16613(7) | 0.32026(9) | 1.36(4) | 0.16(1) | 0.54(2) | 0.57(2) | 3.23 | 7.12 | 1.22 |
| 212.0 | 10.16669(6) | 0.32034(9) | 1.40(4) | 0.14(1) | 0.55(3) | 0.57(3) | 2.84 | 6.07 | 1.49 |
| 225.0 | 10.16679(6) | 0.32028(9) | 1.44(4) | 0.15(1) | 0.59(3) | 0.59(3) | 2.82 | 5.98 | 1.44 |
| 230.0 | 10.16702(7) | 0.32023(9) | 1.44(4) | 0.15(1) | 0.58(3) | 0.57(3) | 2.91 | 6.15 | 1.42 |
| 250.0 | 10.16811(7) | 0.32026(9) | 1.54(4) | 0.17(1) | 0.65(3) | 0.68(3) | 3.21 | 7.04 | 1.07 |
| 300.0 | 10.17063(7) | 0.32017(9) | 1.46(4) | 0.20(1) | 0.71(3) | 0.72(3) | 2.83 | 6.32 | 1.41 |

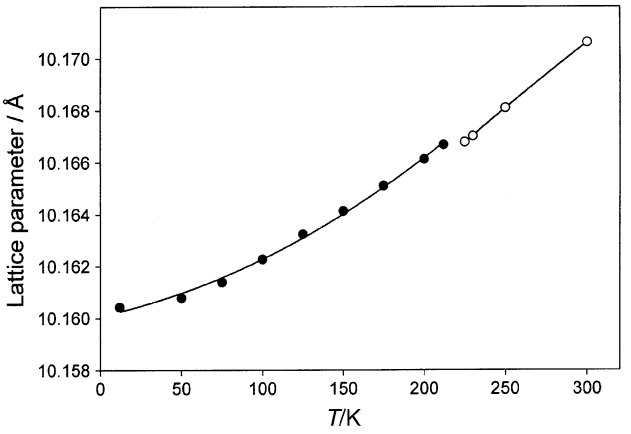


**Fig. 3** Variation of the cubic lattice parameter of $Cd_2Os_2O_7$ between 12 and 298 K. Error bars on the lattice parameter values are within the marker dimensions.

$Tl_2Ru_2O_7$,[5] which has also been investigated by powder neutron diffraction through a $T_{MI}$ transition temperature (142 K, though this material is metallic at low temperatures and semiconducting above $T_{MI}$), only a smooth variation in lattice parameter as a function of temperature is seen. Changes in oxygen positional parameter result in an overall increase in the Ru–O distance and the Ru–O–Ru bond angle at higher temperatures. However, the lack of data points either side of the transition temperature make any difference trends either side of this point difficult to discern.

In terms of the structural parameters, only one position is refineable in the pyrochlore structural model, the O1 $x$ co-ordinate; for a value of 0.3125 this produces perfect $MO_6$ octahedra. The refined value in $Cd_2Os_2O_7$ is around 0.320–0.321 which represents a small trigonal distortion of this unit, producing bond angles around osmium of approximately 93° (×3) and 87° (×3). The variation of this oxygen coordinate as a function of temperature is plotted in Fig. 4 and shows a general decrease with increasing temperature. Coupling the change in this oxygen position with the increasing lattice parameter produces the variations in Os–O bond length in the $OsO_6$ octahedron seen in Fig. 5 and the inter-$OsO_6$ octahedral angle in Fig. 6. At the same time, the $OsO_6$ octahedra become more regular, as shown in Fig. 7, and the Cd–O distances increase, Fig. 8. The overall effect is an unusual, but marked, decrease in the Os–O bond length with increasing temperature (up to the semiconductor to metal transition) associated with an increasing angle between the linked polyhedra. This decrease in bond length is most marked between 125 and 220 K, *i.e.* prior to but not at the semiconductor to metal transition temperature; the plateauing of

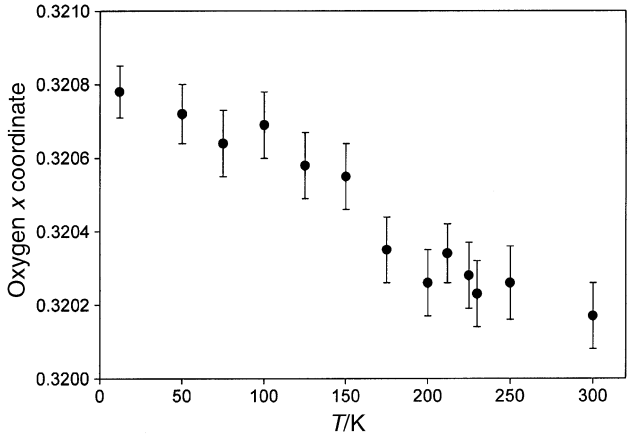


**Fig. 4** Variation of the O1 $x$ co-ordinate between 12 and 298 K.

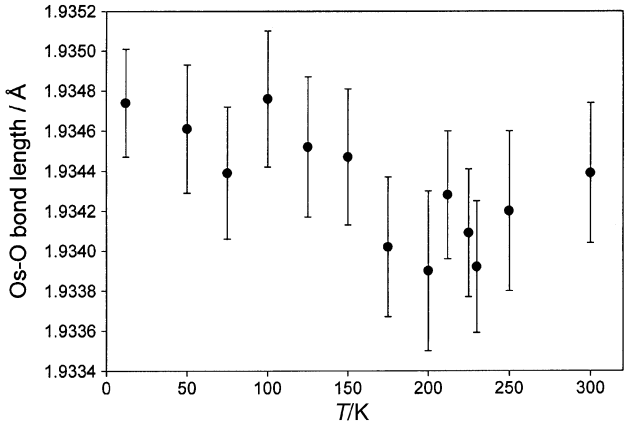


**Fig. 5** Variation of the derived Os–O distance as a function of temperature between 12 and 298 K.

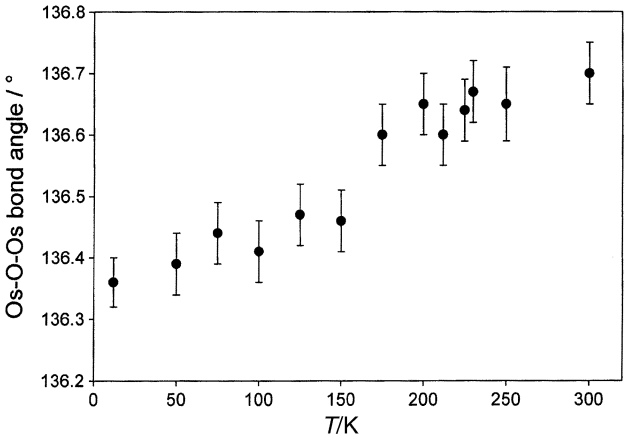


**Fig. 6** Variation of the derived Os–O–Os angle as a function of temperature between 12 and 298 K.

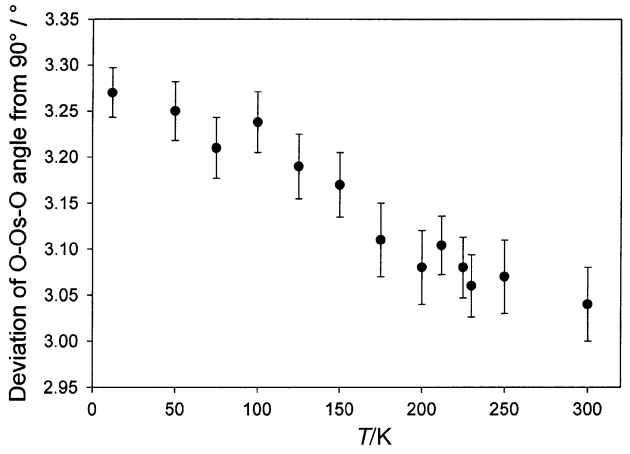


**Fig. 7** Variation of the deviation of the O–Os–O angle from 90° as a function of temperature between 12 and 298 K.

the lattice parameter at 225 K (Fig. 3) has little direct effect on the Os–O bond length (effectively leading to a reduction of less than 0.0002 Å) compared with the overall contraction of over 0.001 Å seen between 12 and 200 K. Above 225 K, the Os–O distance starts to increase as would be expected from thermal expansion considerations.

The evolution of displacement parameters with temperature for the four sites is shown in Fig. 9. The behaviours observed are typical for the pyrochlore structure with notably larger thermal parameters for the "channel" cation, Cd, which may

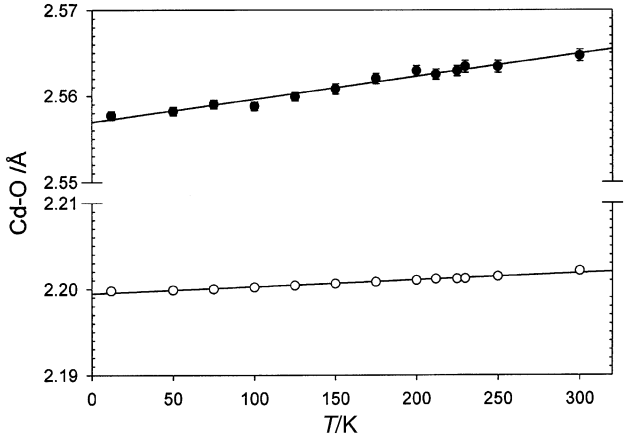


**Fig. 8** Variation of the Cd–O1 (upper) and Cd–O2 (lower) distances as a function of temperature between 12 and 298 K.

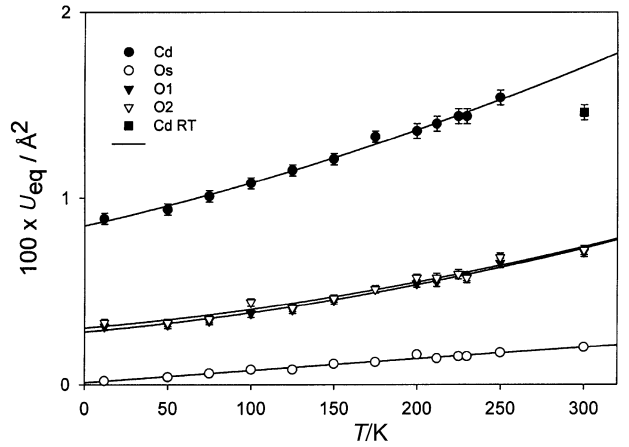


**Fig. 9** Evolution of the thermal parameters of $Cd_2Os_2O_7$ for the individual atom sites between 12 and 298 K

reflect some slight positional disorder. For all sites, a smooth increase is seen throughout the temperature range and any variations near $T_{MI}$ are less than the esds. A slightly anomalous value was obtained for the cadmium site at room temperature, which may be derived from the fact that this point was obtained prior to the sample cooling and heating cycle.

### Magnetic structure

Careful inspection of the large *d*-spacing data collected in the A Bank on POLARIS, Fig. 10, showed that no additional peak appeared on cooling below 225 K, the antiferromagnetic ordering temperature reported by Sleight *et al.*[7] This demonstrates that the magnetic ordering is not long range in nature but must occur locally in the pyrochlore structure. In view of results on other pyrochlores, for example the $R_2Mo_2O_7$ systems,[3,4] this is not surprising as frustrated magnetic behaviour and the formation of spin glass structures for these materials common. In $Y_2Mo_2O_7$, no magnetic scattering is observed below the spin glass transition temperature, a feature that the authors attribute to the small magnetic moment on $Mo^{4+}$. Even where larger magnetic moments are present, *e.g.* $Tb_2Mo_2O_7$, the magnetic scattering is extremely broad and diffuse, and associated with short range antiferromagnetic interactions. The absence of magnetic reflections in the powder pattern of $Cd_2Os_2O_7$, whose presence demands long range three dimensional magnetic order, is thus not unexpected.

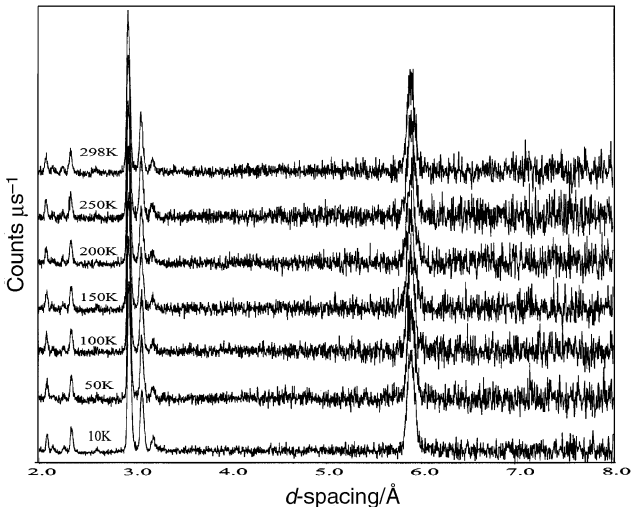


**Fig. 10** Large *d*-spacing data, 2.0 Å $< d <$ 8 Å, from $Cd_2Os_2O_7$ plotted at approximately 50 K intervals between 12 K and room temperature showing no evidence of magnetic reflections.

## Discussion

The transition from semiconducting to metallic behaviour in $Cd_2Os_2O_7$ at 225 K is marked by a small but distinct inflection in the cell parameter, which is reduced with respect to that expected from linear thermal expansion. In terms of structural parameters, the second order nature of the transition is represented by a slow decrease in the Os–O distance up to 225 K, with thermal expansion thereafter. Presumably, the increasing stresses in the system as the osmium to oxygen distances contract and the band gap decreases are relieved suddenly at 225 K with a large drop in resistivity and break in the lattice parameter expansion. Kennedy[2] has investigated structural trends in some Ru and Ir pyrochlores and discussed the results in terms of their electronic structures. The ruthenate pyrochlores can be divided into two classes in respect of their electronic properties in that the Ru–O distances in the metallic ruthenates are lower than those expected on the basis of their lattice parameters and A cation size in comparison with the semiconducting materials. This behaviour has been explained in terms of electron transfer from the 4d bands of ruthenium to the 6s bands of the A-type cation in the metallic regime. Such explanations accord with the behaviour observed in this work on $Cd_2Os_2O_7$. The narrowing and disappearance of the band gap between the Os 5d and Cd 5s on approaching $T_{MI}$ involves transfer of electrons from osmium or, in simple chemical terms, oxidation of Os and reduction of Cd, leading to the observed unusual decrease in the Os–O distances and increase in the Cd–O distances as $T_{MI}$ is approached (Fig. 5 and 9).

The antiferromagnetic ordering below 225 K is localised in nature and does not lead to any magnetic reflections in the diffraction profile above 12 K. Further neutron scattering experiments on our sample of $^{114}Cd_2Os_2O_7$ to investigate the nature of the short range magnetic interactions are planned.

## Acknowledgements

We acknowledge the support of EPSRC for this work under GR/22188 and DERA for studentship funding for J. R.

## References

1 M. A. Subramanian, G. Aravamudan and G. V. Subba Rao, *Prog. Solid State Chem.*, 1983, **15**, 55.
2 B. J. Kennedy, *Physica B*, 1998, **241–243**, 303.
3 J. E. Greedan, J. N. Reimers, C. V. Stager and S. L. Penny, *Phys. Rev. B*, 1991, **43**, 5682.
4 B. D. Gaulin, J. S. Gardner, S. R. Dunsiger, Z. Tun, M. D.

Lumsden, R. F. Kiefl, N. P. Raju, J. N. Reimers and J. E. Greedan, *Physica B*, 1998, **241–243**, 511.
5 Y. Shimakawa, Y. Kubo, T. Mnako, Y. V. Sushko, D. N. Argyriou and J. D. Jorgensen, *Phys Rev B*, 1997, **55**, 6399.
6 M. A. Subramanian, B. H. Toby, A. P. Ramirez, W. J. Marshall, A. W. Sleight and G. H. Kewi, *Science*, 1996, **273**, 81.
7 A. W. Sleight, J. L. Gillson, J. F. Weiher and W. Bindloss, *Solid State Commun.*, 1974, **14**, 357.
8 *Neutron News*, 1992, **3**, 29.
9 A. C. Larson and R. B. von Dreele, Generalised Structure Analysis System, Los Alamos National Laboratory, NM, 1994.
10 J. Rodríguez-Carvajal, S. Rosenkranz, M. Medarde, P. Lacorre, M. T. Fernandez-Díaz, F. Fauth and V. Trounov, *Phys. Rev. B*, 1998, **57**, 456.
11 P. F. Henry and M. T. Weller, to be published in the proceedings of the MRS Fall Meeting 2000.